International Journal of Scientific Research in Science, Engineering and Technology (www.ijsrset.com)
© 2020 IJSRSET | Volume 7 | Issue 3 | Print ISSN: 2395-1990 | Online ISSN : 2394-4099
DOI : https://doi.org/10.32628/IJSRSET207349

Characterization; Formulation and Application of Natural Nano Zeolitic Materials from Kenya as Smart Delivery Systems for Fertilizers and Pesticides

*Gabriel A. Waswa[1], Immaculate N. Michira[1], Debora A. Abong'o[1], Dickson Andala[2], Austin O. Aluoch[3]
[1]Department of Chemistry, University of Nairobi, Nairobi, Kenya
[2]Department of Chemistry, Multimedia University of Kenya, Nairobi, Kenya
[3]Department of Chemical Science and Technology, Technical University of Kenya, Nairobi, Kenya
*Corresponding author's E-mail address: waswagabriel@gmail.com[1]

ABSTRACT

This study aimed at using natural zeolitic materials sampled form different places and characterized as nano porous smart delivery systems for storage and controlled release of fertilizer and pesticide molecules. XRD characterization of sample ZT-GA-01 showed that it was zeolite A artificial, abbreviated as Linde Type A (LTA), sample EL-GA-06 was Phillipsite natural zeolites. IR Spectroscopy for ZT-GA-01 and EB-GA-02 showed similar peaks between 3420 – 3480 cm-1, 2350 – 2360 cm-1 and 1630 – 1660 cm-1 indicating H-O-H stretching and bending, while 440 – 670 cm-1 representing Si-O-Si bending for internal tetrahedral. Besides comparable EDX characterized silica to alumina composition of sample EB-GA-02 and the artificial zeolite A applied as the standard, determined as 37.4 % to 18.8 % and 43.6 % to 56.4 % respectfully. Physical properties of samples ZT-GA-01 and EB-GA-02 in terms of BET surface area, BJH pore volume and pore sizes were obtained as; 0.6716 m2/g, 0.002333 cm3/g, 151.519 Å and 0.7099 m2/g, 0.006767 cm3/g, 389.846 Å respectively. Urea loaded samples EB-GA-02 indicated a 39.844 % reduction in pore sizes after successful loading of urea fertilizer into the nano-spaces, while pesticide loading indicated a reduction in pore volumes and pore sizes by 19.15 % and 32.74 % respectively. The simulated release shoed about 82.8 % of stacked urea fertilizer discharged in water and 74.2 % loaded urea released in soil, while 34.4 % and 40.1 % lambda cyhalothrin pesticide amounts were released by pesticide loaded zeolitic sample EB-GA-02 in water and soil respectively. Application of zeolitic sample EB-GA-02 as smart delivery systems demonstrated a sustained slow release of both urea and Lambda cyhalothrin pesticide on tomato and spinach growing and monitoring experiments for the 60 days' period. In conclusion, our study showed that there exist zeolites and zeolitic materials in some selected parts in Kenya. As well, identified zeolitic sample EB-GA-02 can be used to successfully store agrochemical molecules and significantly delay their release in soil hence applied as nanozeolitic smart delivery systems.

Keywords : Zeolites, Nanopores, fabrication, Smart Delivery Systems

I. INTRODUCTION

To enhance productivity for many decades, uses of fertilizer and pesticides have been applied in the agricultural sector as a measure for sustainable livelihood. Of concern now however, are the counter effects of sustained addition of these chemical components to the environment. Aspects like imbalanced fertilization, decreasing soil organic matter, increasing environmental pollution through processes like leaching, eutrophication, bioaccumulation or otherwise, have a direct correlation to the type and amount of fertilizer and pesticides introduced to the environment, factors that

could hamper the intended increased productivity in the long ran. Besides, a number of researchers (Shaviv, 2000; Chinnamuthu and Boopathi, 2009; Brock *et al*., 2011), have indicated that averagely only 35 % for nitrogen and 20 % for phosphorous fertilizers are actually utilized efficiently by plants. This raises concerns, because it seems that a significant percentage of fertilizer applied is actually not utilized by plants. Meaning, the increased production is not achieved as anticipated and also more chemical pollutant components are continuously added to the environment. To mitigate these dynamics, modern practices are being adopted, many of which integrate the latest line of technological innovations such as the use of Nanotechnology in agriculture, where a great focus on nanostructured formulations of fertilizer and pesticides, through new mechanisms such as target delivery or slow/controlled release, employing carrier agents such as zeolitic materials (materials which contain some percentage of zeolites or having zeolite like properties) could be applied. Usually, they contain crystalline aluminosilicates (Manikandan and Subramanian, 2013) with a series of microporous, mesoporous and nanoporous structures in which ions or molecules can be immobilized through processes like ion exchange and chemisorption mechanisms as a way of loading or encapsulating fertilizer or pesticides to be delivered to plants, while acting as slow/ controlled release process (Chinnamuthu and Boopathi, 2009; Naderi *et al*., (2013). This research focused on formulation of nanozeolitic materials from sampled rocks in selected places within Kenya, characterization and exploration of their applicability on selected fertilizer and pesticide as carrier agents for target delivery or slow/controlled release on selected vegetable production with the intention of enhanced productivity alongside reduced environmental pollution.

II. MATERIALS AND METHODS

Commercial Purchased zeolites (CPZ, from Sigma-Aldrich, P-Code: 101554254, Lot # BCBM 9330V and CAS:1318-02-1.) labeled as sample ZT-GA-01, natural zeolitic rock samples labeled EB-GA-02, MG-GA-03, BG-GA-04, NG-GA-05, EL-GA-06, Urea (analytical standard 99 % pure from IOBA Chemie), Lambda cyhalothrin (analytical standard 99 % pure from IOBA Chemie), Acidified dichromate, Barium chloride, Concentrated Sulfuric acid, Potassium sulfate, Copper sulfate, Selenium sulfate, Concentrated hydrochloric acid, Ammonium acetate, Potassium chloride, Potassium bromide (all analytical standards 99 % pure from IOBA Chemie) and soil sample KIK-GA-01. UV-Visible spectrometer, X-ray diffractometer (XRD, D2 Phaser SSD160 A26-X1-A2DOB2B1, 2nd Gen. from Bruker), Fourier Transform Infrared (FTIR, IR Tracer-100 from Shimadzu), Energy dispersive spectrophotometer (EDS, Shimadzu EDX-720), Analytical balance (Fischer A-160), Orbital shaker (Fischer G-18), Atomic absorbance spectrophotometer (AAS, Perkin Elmer 2100), XRay fluorescence spectrometer (XRF, TITAN 600), Scanning Electron Microscope (SEM, Hitachi S4800), ASAP 2020 Micromeritics equipment, Flame photometer (Sherwood scientific 410), Calcinator (N3A Simon Muller 220V Berlin). Sample EB-GA-02 was collected from Eburru volcanic crater (0.63S, 36.23E), which is located about 8 Km North-West of Lake Naivasha within the Kenyan Rift Valley. Sample MG-GA-03 were collected along the shores of Lake Magadi, as relatively homogeneous bare surface deposits spatially extending 200 m by 10 m. Sample BG-GA-04 were collected on Ol Arabel and Endao seasonal riverbeds near their entry to Lake Baringo. Sample NG-GA-05 was collected from a quarry at Ebul bul (1^0 22'S and $36^0$38'E) near Ngong town in Kajiado County. Sample EL-GA-06 was collected from Kitum caves found at the foot of Mt. Elgon. Sample KIK-GA-01 was collected in Kikuyu area, Kiambu County, at a depth not exceeding 40 cm in arable land, previously having maize and vegetables intergrown,

while sample ZT-GA-01 was commercial zeolitic material samples purchased from Sigma Aldrich. The preparation of the natural zeolitic rock material samples labeled as EB-GA-02, MG-GA-03, BG-GA-04, NG-GA-05 and EL-GA-06 involved mechanical grinding, sieving using 0.85 mm and calcination at 550 °C for 2 hours. KIK-GA-01 and ZT-GA-0 were used as received in all the experiments, without further preparation. Characterization methods included X-Ray Diffraction (XRD), Energy Dispersive X-Ray Spectroscopy (EDX), Fourier-Transform Infrared Spectroscopy (FT-IR), X- Ray Fluorescence Spectroscopy (XRF), Scanning Electron Microscopy (SEM); all followed standard procedures. Soil content analysis and kinetics of fertilizer and pesticide adsorption on zeolitic materials was as reported in our previous publications Waswa *et al.,* 2017(a), Waswa *et al.,* 2017(b), Waswa GA *et al.*, 2018. Modelling efficiency of fertilizer loaded zeolitic materials in crop production procedures involved "pot-set-ups" studied in the form of blank experiments, control experiments and actual monitoring experiments with the crops grown under uniform environmental conditions and crop husbandry practice. Data collection involved determination of the concentration of urea in the soil at a depth of 30 cm over a two months' period, at 5, 20, 30, 45 and 60 days' intervals. Concentration determinations in triplicates were conducted using UV-Spectrophotometry studies. Additional data collection was also done on the physical comparisons of the respective crops in regard to vigor index, size, colour and yield over the entire crop cycle. Efficiency of pesticide loaded zeolitic materials in crop production followed a similar model adopted for fertilizer studies.

III. RESULTS AND DISCUSSION

X-ray diffraction analysis of sample ZT-GA-01(Figure 1) show distinct peaks similar to the ones reported by Treacy *et al.*, (2001), having 2θ values of characteristic artificial zeolite A at 7.2°, 10.3°, 12.6°, 16.2°, 21.8°, 24°, 26.2°, 27.2°, 30°, 30.9°, 31.1°, 32.6°, 33.4° and 34.3°.

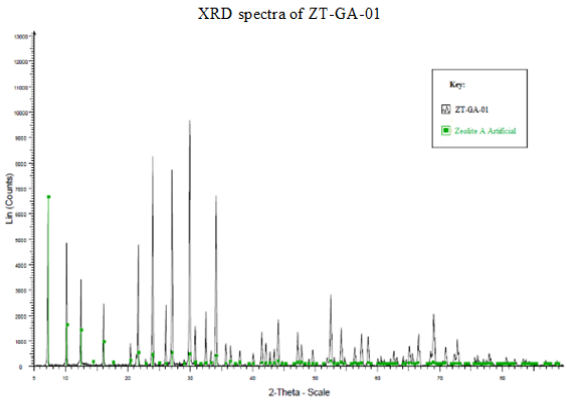

Figure 1: XRD spectra of ZT-GA-01

According to Treacy and Higgins (2001), in their collection of simulated XRD powder patterns for zeolites, zeolite A Artificial is abbreviated as Linde Type A (LTA), having a chemical composition of $[Na_{96}(H_2O)_{216}][Si_{96}Al_{96}O_{384}]$, crystal data of: a = 24.61Å, b = 24.61Å, c = 24.61Å, α=90°, β=90°, γ=90° and X-ray single refinement (Rw) = 0.04, hence the commercial zeolite sample ZT-GA-01 were classified as Zeolite A. Other natural rock samples EB-GA-02, MG-GA-03, BG-GA-04 and NG-GA-05 were analyzed to determine their similarity with sample ZT-GA-01 above. These rocks were characterized while in their natural state after calcination, without any advanced purification process, hence this explains the presence of non-uniform peaks and additional mineral peaks detected.

XRD characterization of zeolitic sample EB-GA-02 gave the characteristic spectrum shown by figure 2.

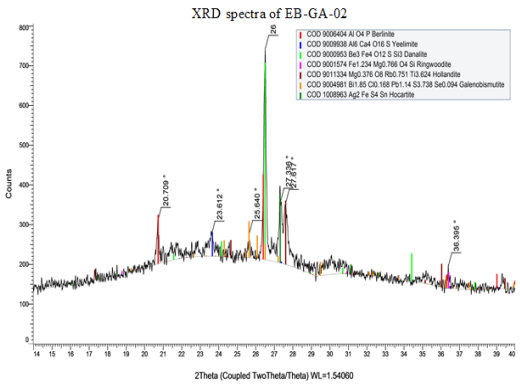

Figure 2: XRD spectra of EB-GA-02

Donalite, Hollandite and Berlinite minerals were found to be the most predominant in this sample at 41.2%, 21.6% and 14.3% respectively.

Figure 3 indicates XRD information generated by sample MG-GA-03.

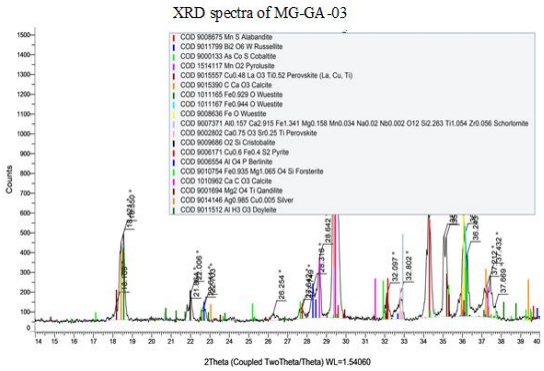

Figure 3: XRD spectra of MG-GA-03

This sample was mainly of trona origin composed of mineral salt calcite. For zeolitic sample BG-GA-04, it's XRD characterization spectrum is shown by figure 4.

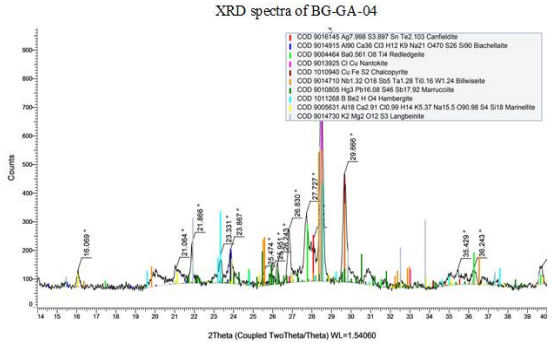

Figure 4: XRD spectra of BG-GA-04

This sample was mainly found to contain Hambergite and Langbeinite minerals at 42.5% and 12.3% respectfully, which are accessory minerals in granite pegmatites.

Analysis of zeolitic sample NG-GA-05 gave the spectrum in figure 5.

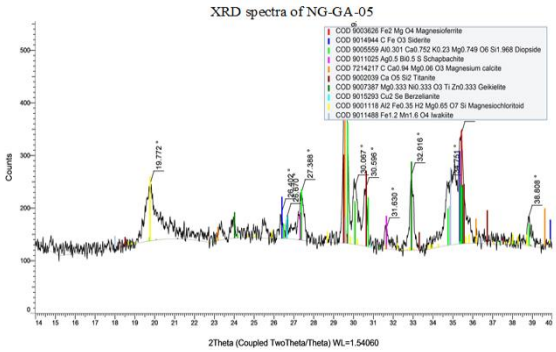

Figure 5: XRD spectra of NG-GA-05

This sample was found to contain Diopside and Titanite minerals in greater quantities.

XRD characterization of zeolitic sample EL-GA-06 generated the spectrum and diffraction parameters recorded in figure 6.

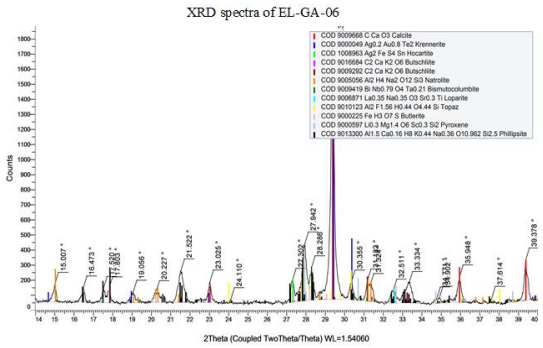

Figure 6: XRD spectra of EL-GA-06

Mineral composition of this sample indicated presence of natural zeolites like Phillipsite, Natrolite and Krennerite. Sample EL-GA-06 was found to be natural zeolites of Phillipsite nature.

Energy Dispersive X-Ray Spectroscopy (EDX) was done to characterize the samples in terms of elemental oxides composition. Zeolite A which was commercially acquired contained mainly oxides of Aluminium and Silicon at 56.000% and 44.000% respectively, as shown by table 1, with its corresponding spectrum (figure 7) below. This was used as standard reference in Energy Dispersive characterization of the other samples.

TABLE I. EDX QUANTITATIVE RESULTS OF SAMPLE ZT-GA-01

Analyte	Result %	Standard Deviation	Intensity (cps/uA)
Al_2O_3	56.368	1.335	0.0721
SiO_2	43.632	0.398	0.4315

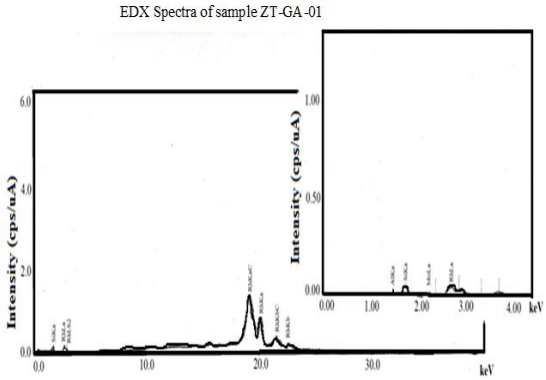

Figure 7: EDX Spectra of sample ZT-GA-01

Characterization of sample EB-GA-02 indicated oxides of Aluminium and Silicon at 18.8 % and 37.4 % respectively, alongside other oxides like of Fe and K. Multiple peaks corresponding to the present elements are illustrated by the spectrum in figure 8 below.

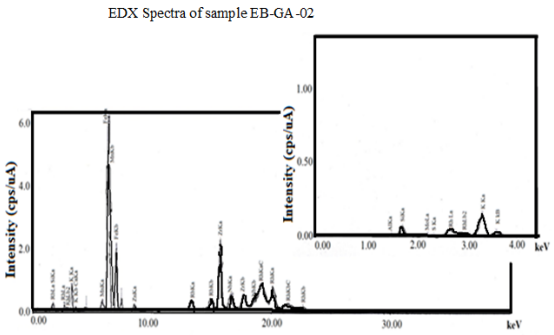

Figure 8: EDX Spectra of sample EB-GA-02

Fourier-Transform Infrared spectra of the zeolitic samples ZT-GA-01, EB-GA-02, MG-GA-03, BG-GA-04 and NG-GA-05 were scanned in the mid and far (4000-400cm^{-1}) infrared regions to generate distinct peaks as assigned in table 2 below. According to Clark *et al.*, 2004, strong fundamental vibrations of the alumino silicate framework of minerals and glasses, as well as the principal vibration modes of most molecular species like Si-O, C-O, S=O and P-O are located in the mid IR-region. (Can *et al.*, 2003, Wlodzimier *et al.*, 2011, Sitarz *et al.*, 1997, Mozgawa *et al.*, 2005).

TABLE II. AN OVERVIEW OF INFRARED BAND POSITIONS OF STUDIED ZEOLITIC MATERIALS

Wavenumbers (cm^{-1})					Assignments
ZT-GA-01	EB-GA-02	MG-GA-03	BG-GA-04	NG-GA-05	
3471.87	3421.72	3421.72	3421.72	3444.87	H-O-H Stretching of absorbed water (Mozgawa *et al.*, 2005)
-	-	2924.09	2924.09	2924.09	C-H Stretching
2357.01	2360.87	2360.87	2360.87	2360.87	-
1654.92	1635.64	1774.51	1774.54	-	H-O-H Bending of water
-	-	1438.90	1438.90	1435.04	C-H Stretching
-	-	1033.85	1033.85	1037.70	Si-O Assymetric stretch for internal tetrahedral (Sitarz *et al.*, 1997)
-	-	875.68	875.68	-	OH Deformation linked to $2Al^{3-}$ (Wlodzimier *et al.*, 2011)
-	786.96	702.09	702.09	775.38	Si-O quartz (Wlodzimier *et al.*, 2011)
663.51	-	-	-	-	Si-O-Si Bending (Can *et al.*, 2003)
-	447.49	-	-	-	Si-O-Si Bending for internal tetrahedral (Can *et al.*, 2003)

X-Ray Fluorescence spectroscopy (XRF) summary of data for all the analysed indicated that sample ZT-GA-01, which was used as the standard, being zeolite A obtained commercially had very low concentration units of the listed elements. Cu at 148 ppm was detected as the highest concentration of impurities, followed by Ti at 127 ppm and Mn at 82.1 ppm. Most of the other impurities like Pb, Nb, Y and Rb were below 5ppm. Additionally, this sample had percent by weight of less than 0.08 of K, Ca and Fe elements, which indicates a high level of purity of the commercial zeolites. Comparatively, sample EB-GA-02 had the highest composition of Ti impurities at 2478ppm, Mn at 2358ppm, Zr at 2111 ppm and Cu at 1901 ppm, while the other impurities like Pb, Nb, Y and Rb mostly being below 300ppm. This sample had percent by weight between 0.3 – 7.00 of K, Ca and Fe elements. Hence, effective purification process could improve the extent of zeolitic comparability to sample ZT-GA-01, if carried out, process that was beyond the scope of this current research work.

Scanning Electron Microscopy (SEM) images provided information on sample surface morphology and particle sizes. Sample ZT-GA-01 which was artificial commercial zeolite A showed aggregated cubical particles of uniform sizes (Figure 9).

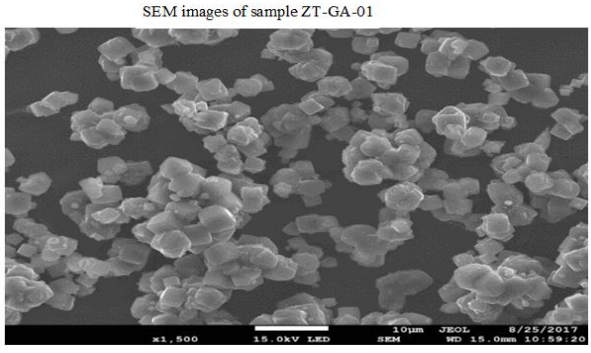

Figure 9: SEM images of sample ZT-GA-01

They had better defined crystals with regular shapes, which seemed to have well-developed structures on surface and converged particles. These are similar observations made by Pereira *et al.* (2012) and Mohanraj (2013). This could probably be due to high levels of crystal purity. The rest of the samples had non uniform surface morphologies and particle sizes (Figure 10). These SEM images were from raw natural zeolitic materials which would have probably given more elaborate images on purification and particle reduction processes.

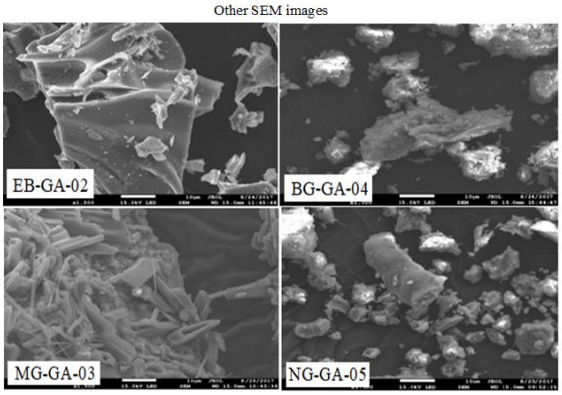

Figure 10: Other SEM images

Nitrogen adsorption-desorption isotherm of commercial zeolite sample ZT-GA-01 and natural zeolitic rock sample EB-GA-02 are presented in figure 11 below. These isotherms show variation in adsorption between pressures below 0.2, 0.3 - 0.6 and above 0.8, giving a similarity to type IV isotherm commonly shown by mesoporous materials (Sing *et al.,* 1985). At relatively higher pressure desorption levels, there is formation of narrow hysteresis loops which could be associated with mesopore capillary condensation. Pressure zon 0.3 – 0.6 could represent completion of monolayer coverage and formation of multilayer process. Physical properties of samples ZT-GA-01 and EB-GA-02 in terms of BET surface area, BJH pore volume and pore sizes were obtained as; 0.6716 m^2/g, 0.002333 cm^3/g, 151.519 Å and 0.7099 m^2/g, 0.006767 cm^3/g, 389.846 Å respectively. Urea loaded samples EB-GA-02 indicated a 39.844 % reduction in pore sizes after successful loading of urea fertilizer into the nano-spaces, while pesticide loading indicated a reduction in pore volumes and pore sizes by 19.15 % and 32.74 % respectively.

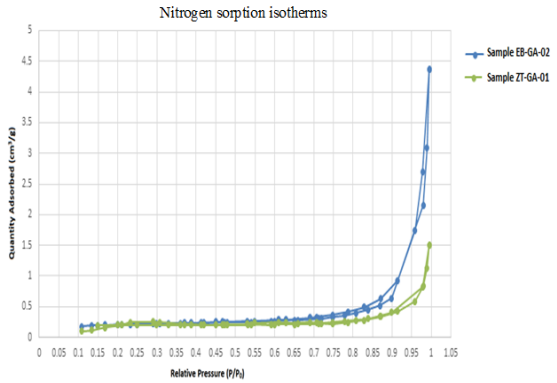

Figure 11. Nitrogen sorption isotherms of samples ZT-GA-01 and EB-GA-02.

The results and discussions on kinetics of fertilizer and pesticide sorption on zeolitic materials were as reported in our initial work Waswa *et al.,* 2017(a) and Waswa *et al.,* 2017(b). Results of Loading of fertilizer into zeolitic materials showed X-Ray diffraction analysis of urea loaded sample EB-GA-02 (Figure 12) indicated 2θ peaks values of 22, 24.5, 29.5, 32, 35.5, 37, 38.5, 40.5, 41.5, 45.5 and 55 corresponding to urea peaks.

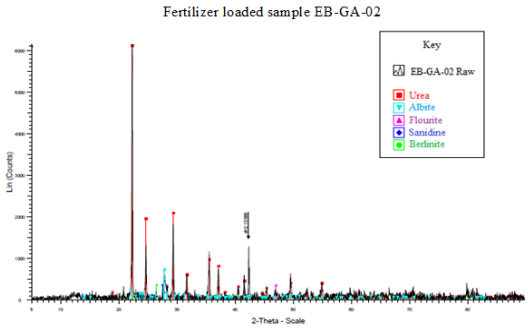

Figure 12: Fertilizer loaded sample EB-GA-02

Fourier Transform Infrared analysis of urea fertilizer showed major peaks at 3348.42-3444.87cm^{-3}, 1624.06-1681.93cm^{-3} and 1465.90cm^{-3} corresponding to N-H, C=O and C-N functional groups respectively (Stuart, 2004). The spectrum of Urea loaded sample EB-GA-02 below (figure 13) contained distinct peaks appearing on the urea spectrum at 3348.42-3444.87cm^{-3}, 1624.06-1681.93cm^{-3} and 1465.90cm^{-3}, corresponding to N-H, C=O and C-N stretching vibrations for the urea fertilizer functional groups respectively. The SEM image obtain are shown by figure 14.

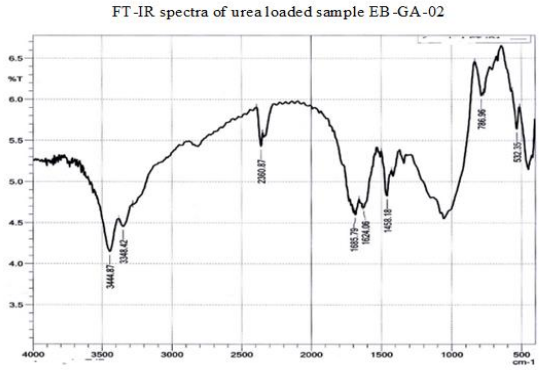

Figure 13: FT-IR spectra of urea loaded sample EB-GA-02

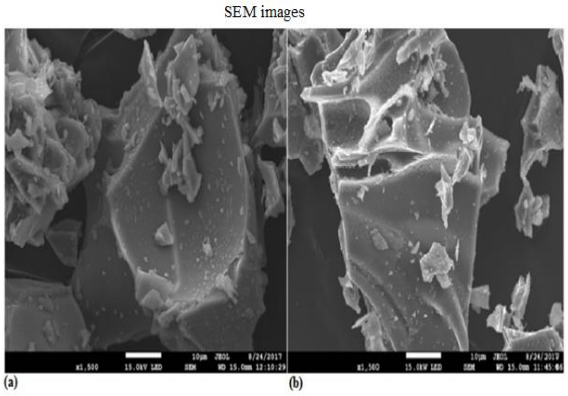

Figure 14: SEM images of (a) urea loaded sample EB-GA-02 (b) blank sample EB-GA-02

Controlled release behavior of fertilizer loaded zeolitic materials EB-GA-02 in water had 82.8 % and 74.2% in soil. Urea loaded sample KIK-GA-01 had 0.071309 moldm^{-3} at 58.9% desorption discharge rate, a low percentage likely due to high organic carbon content with stronger binding forces, all with a rapid initial and then steady sustainable rate. These comparative discharge for urea loaded sample EB-GA-02 in aqueous medium, in Kikuyu soil and in aqueous medium was presented by 'a', 'b' and 'c' respectively in the 'key' for figure 15 where urea loaded sample KIK-GA-01 had the least discharge amount of urea in aqueous medium. Beyond the 12 days, the bars of discharge of urea loaded sample EB-GA-02 in aqueous medium was higher proportionally than the others. This implies that loading urea fertilizer into sample EB-GA-02 and applying the same as carrier agents had a better sustained release rate, which could still

avail the minimum remaining fertilizer to the crops for slightly longer duration than the direct application.

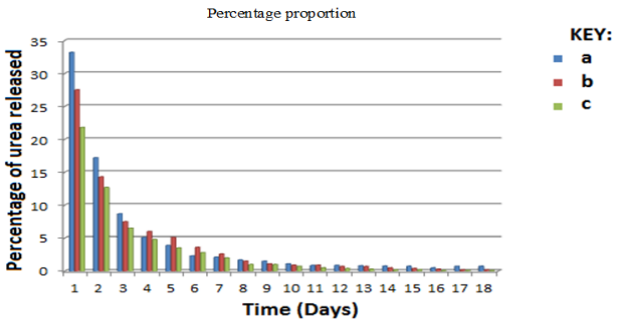

Figure 15: Percentage proportion variation of urea release

Efficiency of fertilizer loaded zeolitic materials in crop production showed urea loaded zeolitic sample EB-GA-02 having a sustained slower but extended releases rate when applied for tomato monitoring (Figure 16) and spinach monitoring (Figure 17). In both of these figures, it was observed that the graph of urea loaded zeolitic sample EB-GA-02 initially had a lower concentration, but beyond the 25th day, they recorded slightly higher concentration compared to concentration determined by direct fertilizer application. For tomato studies, urea loaded zeolitic sample EB-GA-02 gave a difference of almost 17.00% higher concentration, while a difference of about 16.00% higher concentration was recorded on spinach between the 25th and 35th.

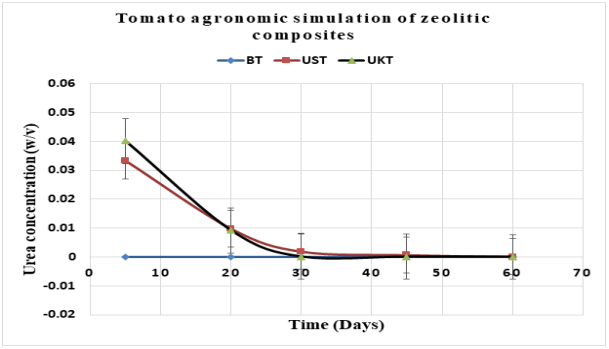

Figure 16: Comparative slow release rates for urea loaded zeolitic materials in tomatoes studies

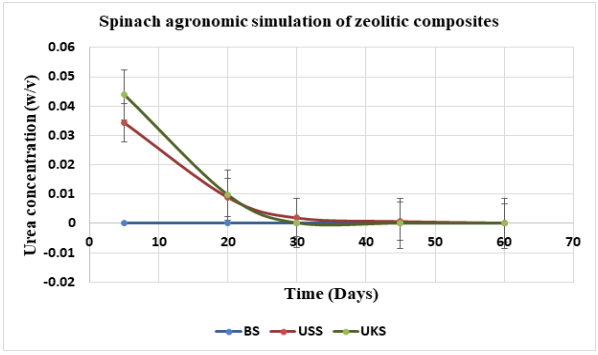

Figure 17: Comparative slow release rates for urea loaded zeolitic materials in spinach studies

Therefore, these observations indicate that it is possible to apply urea loaded zeolitic sample EB-GA-02 as carrier agent for urea fertilizer in which the rate of delivery of urea molecules to both tomato and spinach can be monitored. The sustained concentration of urea in the soil over the entire monitoring duration indicated slow delivery process which helps avail the urea nutrients to the plant over a longer duration.

Loading of pesticides into the zeolitic materials indicated that, 79.4% of Lambda cyhalothrin pesticide was loaded in the weighed mass of the sample EB-GA-02. Confirmation of loading the pesticide molecules into the samples was done using X-Ray diffraction and Fourier Transform Infrared analysis. X-ray diffraction analysis of Lambda cyhalothrin pesticide loaded sample EB-GA-02 (figure 18) indicated the pesticide 2θ values at 28.5, 33, 47, 56, 58.5, 68.5, 76, 78 and 87 degrees.

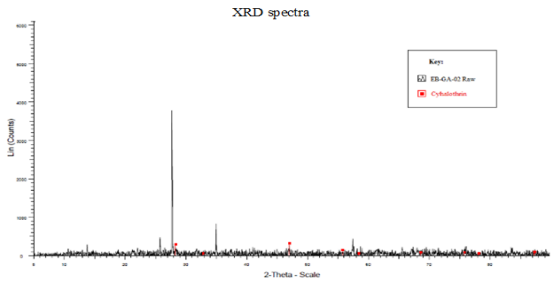

Figure 18: XRD spectra of pesticide loaded sample EB-GA-02

While FT-IR analysis gave the spectrum shown in figure 19 below, with peaks corresponding to some of the functional groups present in Lambda cyhalothrin molecule. The corresponding SEM images are shown by figure 20.

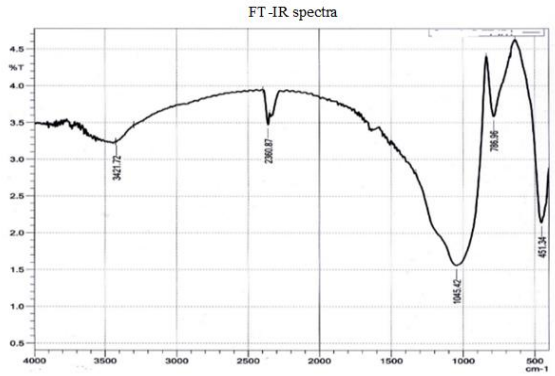

Figure 19: FT-IR spectra of pesticide loaded sample EB-GA-02

From the Infrared spectrum, some specific peaks associated with some functional groups present in Lambda cyhalothrin structure can be identified. These includes 3695.61cm^{-1} associated with C-H stretching in heterocyclic compounds,1635.64cm^{-1} for esters, 1037.7 cm^{-1} for C-O stretching in ethers and 794.67 cm^{-1} that could be associated with C-F stretching for halogen substituted organic compounds (Stuart, 2004).

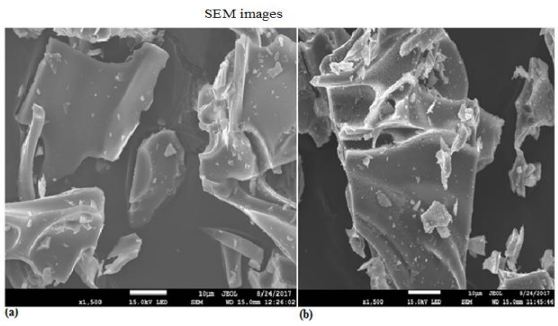

Figure 20: SEM images of (a) pesticide loaded sample EB-GA-02 (b) blank sample EB-GA-02

Comparative discharge studies were conducted between the pesticide loaded sample EB-GA-02 in aqueous medium, pesticide loaded sample EB-GA-02 in Kikuyu soil and finally pesticide loaded sample KIK-GA-01 in aqueous medium. The results obtained were represented in figure 21. The rate of discharge of the pesticide loaded zeolitic materials in aqueous medium was the highest as seen by graph x having the steepest initial gradient. This could be attributes to very low organic matter content present in these natural rock materials, hence exhibiting low physicochemical interaction between the Lambda cyhalothrin molecules and the sorption sites of the rock.

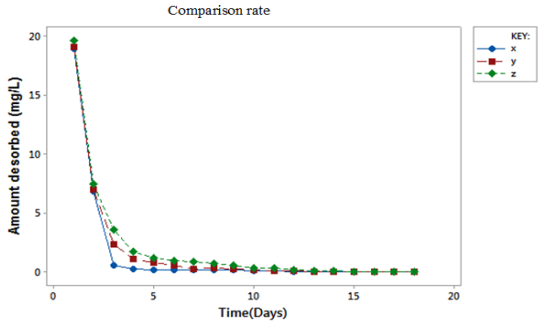

Figure 21: Comparison rate of pesticide release (Where x represents pesticide loaded

EB-GA-02 release in aqueous medium, y represents pesticide loaded sample EB-GA-02 mixed with soil from Kikuyu and z represents pesticide loaded sample KIK-GA-01release in aqueous medium. Pesticide loaded Kikuyu soil (sample KIK-GA-01) had the least discharge of the loaded pesticide in aqueous medium as represented by 'z' illustrated by plots and the bar chart in figure 22. This soil had higher carbon content at 2.7%, with more silt and clay medium in it, which could imply a relatively higher physicochemical interaction between the Lambda cyhalothrin molecules and the soil particles. This implies that more pesticide molecules were retained by the soil molecules and matrix.

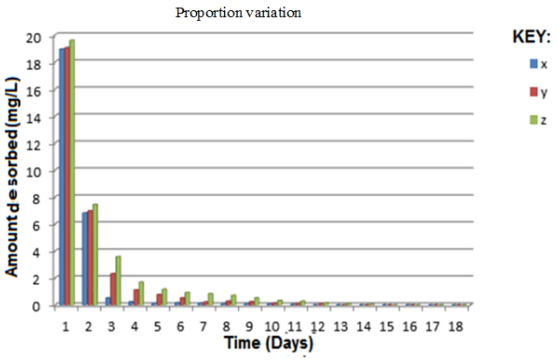

Figure 22: Proportion variation of pesticide release (Where x represents pesticide loaded sample EB-GA-02 release in aqueous medium, y represents pesticide loaded sample EB-GA-02 mixed with soil from

Kikuyu and z represents pesticide loaded sample KIK-GA-01 release in aqueous medium).

Efficiency of pesticide loaded zeolitic materials in crop production for tomatoes monitoring studies indicated a sustained slow decrease when pesticide loaded zeolitic sample EB-GA-02 were applied as compared to direct application of the pesticide (Figure 23).

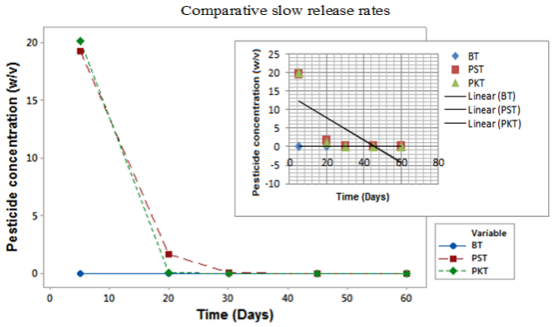

Figure 23: Comparative slow release rates for pesticide loaded zeolitic materials in tomatoes studies

Initially, there was more pesticide in the soil where direct application was done, mainly over the first 10 days, but around the 20th day, a higher concentration of Lambda cyhalothrin which was more than fivefold, was recorded for the soils in the experiments done using pesticide loaded zeolitic sample EB-GA-02 at almost 70% difference.

Similar trends were observed when it came to spinach studies. Generally, over the 60 days duration, there was a more sustained release of Lambda cyhalothrin pesticide into the soil by the pesticide loaded sample EB-GA-02 (Figure 24). Higher concentration amounts were noted in the soil, particularly from the 15th day to the 35th day, with a 69% highest value recorded around the 30th day. These findings reinforced the idea of sustained and controlled release of pesticide molecules by the zeolitic loaded samples. Hence, zeolitic samples EB-GA-02 were successfully used as smart delivery systems for lambda cyhalothrin pesticide when applied to both tomatoes and spinach studies.

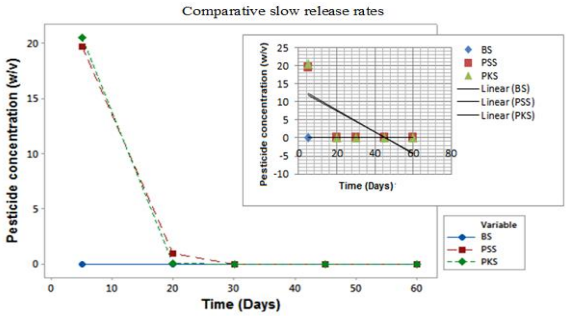

Figure 24: Comparative slow release rates for pesticide loaded zeolitic materials in spinach studies

IV. CONCLUSION

Zeolitic materials labeled EB-GA-02, MG-GA-03, BG-GA-04, NG-GA-05 and EL-GA-06 were explored from five different sites in Kenya and characterized using XRD, XRF, EDX and FT-IR compared to artificial zeolite A (sample ZT-GA-01) as the standard. Sample EL-GA-06 was found to be mainly natural zeolite Phillipsite with some Nitrolite deposits; sample EB-GA-02 had a higher favourable similarity in silica and alumina ratio to the standard, besides it's morphological properties like porosity and large quantity deposits that made it preferred for nanozeolitic formulation for smart delivery system. Formulation nanozeolitic smart delivery system indicated that 35.00 % of urea fertilizer and 79.40 % of Lambda cyhalothrin pesticide were loaded separately in the nonopore spaces of the sample EB-GA-02 forming urea loaded nanozeolitic sample EB-GA-02 and pesticide loaded nanozeolitic sample EB-GA-02 smart delivery systems. Simulation studies showed 82.80% and 74.20% of loaded urea molecules were separately released in water and soil respectfully, while 34.40% and 40.10% of the loaded Lambda cyhalothrin molecules were separately released in soil and water respectfully. Urea loaded nanozeolitic smart delivery system samples demonstrated a sustained slower but extended release rate when applied to both tomatoes and spinach crops. A difference of 17.00% and 16.00% higher urea concentration in soil was recorded on tomatoes and spinach crops respectfully between the 20th and 35th day as compared to just direct urea application to the

soil. Similarly, pesticide loaded nanozeolitic smart delivery system samples gave a difference of 70.00% and 69.00% higher Lambda cyhalothrin pesticide concentration in soil recorded for tomatoes and spinach respectfully around the 20th day for each. These observations demonstrated the application of nanozeolitic sample EB-GA-02 in formulation of nanosmart delivery system that can aid in slow and controlled release and delivery of fertilizer and pesticide to crops.

IV. ACKNOWLEDGEMENT

I would like to acknowledge the National Commission for Science, Technology and Innovation (NACOSTI) and the National Research Fund (NRF) for their Endowment Funds for this Project. The following institutions availed instruments for various analysis: State Department of Infrastructure Material Testing and Research Division in Kenya, Mines and Geology Department in Kenya, Kenya Agricultural and Livestock Research Organization, University of Nairobi College of Biological and Physical Sciences and St. Austin's Academy Chemistry Laboratory. The following people provided their special support that helped to obtain project objectives: Dr. A. K. Waswa from Department of Geology, UoN for your insights on zeolites, Mr. J. K. Mbugua PhD student from Chemistry Department UoN for being part of my research team and hosting my field work studies, Mr. J. Njoroge from Infrastructure Material Testing and Research Division for facilitating some of our laboratory works.

V. REFERENCES

[1]. Brock, D. A., Douglas, T.E., Queller, D. C. & Strassmann, J. E. (2011). Primitive agriculture in a social amoeba. Nature 469: 393-396.

[2]. Can, L. & Zili, W. (2003). Microporous Materials Characterized by Vibrational Spectroscopies. In Handbook Zeolite Scie. CRC Press, 2003.

[3]. Chinnamuthu, C. R. & Boopathi, P. M. (2009). Nanotechnology and Agroecosystem. Madras Agricultural Journal 96:17-31.

[4]. Clark, R. N. (2004). Spectroscopy of rocks and minerals, and principles of spectroscopy. In Infrared Spectroscopy in Geochemistry Exploration. Geochemistry and Remote Sensing. Mineral Association Canada, Short course, 33, 17-35.

[5]. Manikandan, A. & Subramanian, K. S. (2014). Fabrication and characterisation of nanoporous zeolite-based N fertilizer. African Journal of Agricultural Research. Vol. 9(2), pp. 276-284, 9 January.

[6]. Mohanraj, J. (2013). Effect of nano-zeolite on nitrogen dynamics and greenhouse gas emission in rice soil eco system M.Tech. Thesis, Tamil Nadu Agricultural University, Coimbatore.

[7]. Mozgawa, W., Jastrzebski, W. & Handke, M. (2005). Vibration Spectra of D4R and D6R Structural Units. Journal of Molecular Structures. 744-747, 663-670.

[8]. Naderi, M. R. & Danesh-Shahraki, A. (2013). Nanofertilizers and their role in sustainable agriculture. International Journal of Agriculture and Crop Sciences: vol 5 (19): 2229-2232.

[9]. Pereira, E. I., Minussi, F. B., Cruz, C. C. T., Bernardi, A. C. C., & Ribeiro, C. (2012). Urea–Montmorillonite-Extruded Nanocomposites: A Novel Slow-Release Material. J. Agric. Food Chem., 60: 5267–5272.

[10]. Shaviv, A. (2000). Advances in Controlled Release of Fertlizers. Advanced Agronomy Journal 71: 1-49.

[11]. Sitarz, M., Mozgawa, W. & Handke, M. (1997). Vibration spectra of complex ring silicate anions method of recognition. Journal of molecular structure. Vol. 404: 193-197.

[12]. Sing, K. S. W., Everett, D. H., Haul, R. A. W., Moscou, L., Pierotti, R. A., Rouquerol, J. & Siemieniewska T. (1985). Reporting

[13]. physisorption data for gas/solid systems with special reference to the determination of surface

area and porosity. Pure Appl. Chem. 57: 603 - 619.

[14]. Stuart, B. (2004). Infrared Spectroscopy: Fundamentals and Applications © 2004 John Wiley & Sons, Ltd. ISBN: 0-470-85427-8 (HB); 0-470-85428-6 (PB).

[15]. Treacy, M. J. & Higgins, J. B. (2001). Collections of Simulated XRD Powder Patterns for Zeolites, 4th ed. Elsevier, Amsterdam, The Netherlands, 379 p.

[16]. Waswa, G. A., Andala, D., Aluoch, A. O., Kamau, G. N. & Michira, I. (2017). APPLICATION OF EBURRU ROCKS FROM KENYA AS UREA CARRIER AGENTS. International Journal of Recent Advances in Multidisciplinary Research: Vol. 04, Issue 04, pp.2532-254.

[17]. Waswa, G. A., D. Andala, A. O. Aluoch, G. N. Kamau, I. Michira & J. K. Mbugua (2017).

[18]. Kinetics and Isothermal studies of Lambda Cyhalothrin sorption on Eburru soil in Kenya. Journal of the Kenya Chemical Society: 10-1, 24-34.

[19]. Waswa, G. A., Michira I, Abong O, Mbugua J. K. & Andala, D. (2018). Dissipation and Sorption of Urea on Eburru Soils in Kenya. J Phys Chem Biophys 7: 271.

[20]. Wlodzimier, M., Magdalena K. & Kataryzana, B. (2011). FT-IR of zeolites from different structural groups. CHEMIK 65 (7): 667-674.

Cite this article as :

Gabriel A. Waswa, Immaculate N. Michira, Debora A. Abong'o, Dickson Andala, Austin O. Aluoch, "Characterization; formulation and application of Natural Nano zeolitic materials from Kenya as Smart Delivery Systems for fertilizers and pesticides", International Journal of Scientific Research in Science, Engineering and Technology (IJSRSET), Online ISSN : 2394-4099, Print ISSN : 2395-1990, Volume 7 Issue 3, pp. 338-349, May-June 2020. Available at doi : https://doi.org/10.32628/IJSRSET207349
Journal URL : http://ijsrset.com/IJSRSET207349